

FIRE MODELLING STANDARDS/BENCHMARK

Report on SMARTFIRE Phase 2 Simulations

by

A.J.Grandison, E.R.Galea and M.K.Patel

**Fire Safety Engineering Group.
University of Greenwich
London SE10 9LS.**

for

**Dr David Peace
Head
Fire Research And Development Group.
Home Office.**

MAY 2001.

Contents

EXECUTIVE SUMMARY	3
1.0 INTRODUCTION.....	5
2.0 BACKGROUND.....	5
3.0 THE PHASE 2 RESULTS.....	6
3.1 CFD CASES.....	7
3.1.1 SMARTFIRE: 2000-1-5 RADIATION IN A 3D CAVITY.....	7
3.2 FIRE CASES	12
3.2.1 SMARTFIRE: 2000-2-1 – STECKLER FIRE CASE.....	12
3.2.2 SMARTFIRE: 2000-2-5 – LPC007 CASE.....	19
CONCLUDING COMMENTS.....	26
REFERENCES.....	28

EXECUTIVE SUMMARY

The purpose of the proposed standards/benchmarks is to aid the fire safety approvals authority in assessing the appropriateness of using a particular model for a particular fire modelling application. This benchmarking exercise has been split into two phases. The first phase was intended to test all the participating software products (i.e. PHOENICS, CFX and SMARTFIRE) using identical or equivalent models, which were a subset of the full range of the software capability, against standard test scenarios. The second phase of testing allowed the full range of the software's capability to be demonstrated.

In studying the outcome of the Phase 1 test cases, it was clear that when identical physics modelling is activated, identical computational meshes used and similar convergence criteria applied, all of the software products (PHOENICS, CFX and SMARTFIRE) tested were capable of generating similar results. This is an important observation and suggests – within the limitations of the tests undertaken – that these three software products have a similar basic capability and are capable of achieving a similar basic standard. While there were minor differences between the results generated by each of the software products; on the whole they produce – for practical engineering considerations – identical results. From a regulatory viewpoint, it is reassuring to have an independent verification of this similarity.

A significant – and somewhat reassuring - conclusion to draw from these results is that an engineer using the basic capabilities of any of the three software products tested would be likely to draw the same conclusions from the results generated irrespective of which product was used. From a regulators view, this is an important result as it suggests that the quality of the predictions produced are likely to be independent of the tool used – at least in situations where the basic capabilities of the software are used.

Only one of the software producers chose to participate in Phase 2, namely SMARTFIRE. The Phase 2 testing has now been successfully completed and this report details the findings. In studying the outcome of the Phase 2 test cases, it is clear that by activating sophisticated physical models, the software product tested was capable of generating improved predictions against theoretical and experimental data in all of the cases examined. While this may seem an intuitively obvious result, it is a necessary demonstration of the capability of the fire modelling tool that this occurs in a measurable and reproducible manner.

Furthermore, these results should not be treated in isolation but taken within the context of the Phase 1 findings. A significant conclusion from the Phase 1 predictions was that within the limits of the Phase 1 testing regime and taking into consideration experimental inconsistencies and errors, all three Software Products (SPs) were capable of producing reasonable engineering approximations to the experimental data, both for the simple CFD and fire cases. With the completion of the Phase 2 testing, this statement is somewhat strengthened - at least for the software product tested in Phase 2.

The concept and testing protocols developed as part of this project have been shown to be a valuable tool in providing a verifiable method of benchmarking and gauging the basic

capabilities of CFD based fire models on a level playing field. To further improve the capabilities of the approach, it is recommended that additional test cases in the two categories be developed, several of the fire cases be refined, and the testing protocols modified so that the software product developers undertake the bulk of the testing and the testing organisation perform the spot/random checks.

It is finally recommended that the principles and procedures produced in this project be further developed to provide a quality measure of fire modelling software that is used in the U.K. for design purposes.

1.0 Introduction

The Fire Modelling Standards/Benchmark (FMSB) project marks the first step in the development of a set of standards/benchmarks that can be applied to fire field models. The project is led by the University of Greenwich's Fire Safety Engineering Group ([FSEG](#)) and funded by the [Home Office Fire Research and Development Group](#), now part of the DTLR. It is not the intent of the current phase of this project to definitively define the entire range of standards/benchmarks but to suggest and demonstrate the principle behind the proposed standards and to propose the required next steps. It is expected that the suite of benchmark test cases will evolve over time as suitable new experimental data is made available or as new theoretical cases are developed.

The ultimate purpose of the proposed standards/benchmarks is to aid the fire safety approvals authority e.g. fire brigade, local government authority, etc in assessing the appropriateness of using a particular model for a particular application. Currently there is no objective procedure that assists an approval authority in making such a judgement. The approval authority must simply rely on the reputation of the organisation seeking approval and the reputation of the software being used. In discussing this issue it must be clear that while these efforts are aimed at assisting the approval authorities, there are in fact three groups that are involved, the approvals authority, the general user population and the model developers. Ideally, the proposed standards/benchmark should be of benefit to all three groups. In proposing the standards/benchmark, it is not intended that meeting these requirements should be considered a SUFFICIENT condition in the acceptance process, but rather a NECESSARY condition. Finally, the benchmarks are aimed at questions associated with the software, not the user of the software.

This benchmark process has been split into two phases. The first phase is intended to test all the software products using identical or equivalent physical models, convergence requirements and computational meshes. The second phase of testing allows the full range of the software's capability to be demonstrated.

This document marks the conclusion of the second phase of the project, the performance of the phase 2 simulations. Results for the phase 2 simulations are presented along with a discussion of the results. The broad definition of the Phase 1 and Phase 2 simulations may be found in Appendix A with the precise definition of the phase 2 problems for each of the software products being defined in Appendix C, D and E.

2.0 BACKGROUND

The first phase of the testing programme has been successfully completed and a report published [1] which is also available on the FSEG web site [2]. In studying the outcome of the Phase 1 test cases, it was clear that when identical physical models are activated, identical computational meshes used and similar convergence criteria applied, all of the software products (PHOENICS [3], CFX [4] and SMARTFIRE [5]) tested are capable of generating similar results. This is an important observation and suggests – that within the limitations of the tests undertaken – that these three codes have a similar basic capability

and are capable of achieving a similar basic standard. While there are minor differences between the results produced by each of the software products, on the whole they produce – for practical engineering considerations – identical results. From a regulatory viewpoint, it is reassuring to have an independent verification of this similarity.

The one area that showed relatively poor agreement between model predictions and theoretical results concerned the six-flux radiation model performance. The six-flux radiation model while capable of representing the average trends of radiative heat transfer within the compartment, does not produce an accurate representation of local conditions.

A significant – and somewhat reassuring - conclusion to draw from these results is that an engineer using the basic capabilities of any of the three software products tested would be likely to draw the same conclusions from the results generated irrespective of which product was used. From a regulators view, this is an important result as it suggests that the quality of the predictions produced are likely to be independent of the tool used – at least in situations where the basic capabilities of the software are used.

A second significant conclusion is that within the limits of the tests cases examined and taking into consideration experimental inconsistencies and errors, all three software products are capable of producing reasonable engineering approximations to the experimental data, both for the simple Computational Fluid Dynamics (CFD) cases (i.e. non-fire cases) and full fire cases.

The concept of the Phase 1 testing protocols has been shown to be a valuable tool in providing a verifiable method of benchmarking and gauging the basic capabilities of CFD based fire models on a level playing field. To further improve the capabilities of the approach, it is recommended that additional test cases in the two categories (basic CFD non-fire and fire) be developed. It is however vital to note that for results to be officially considered part of this benchmark, they must go through the established process.

3.0 The Phase 2 Results

This section contains the results from the Phase-2 testing regime. The CFD and fire cases were designed to test the basic features of the SP to ensure that these functioned correctly.

In Phase-1, testing was designed to ensure that the codes are set up as similarly as possible. This includes using the same computational mesh and physics models. In Phase-2, the participants were free to optimise the set-up of each of the test cases. This means that the mesh can be refined and more sophisticated physics routines that are available within the codes can be activated. In addition, participants were free to select which of the test cases they wish to repeat. However, all software set-ups must be reported so that they can be repeated. Details of the numerical set-ups for the phase 2 CFD and fire cases can be found in Appendix C, D and E. Details of the set-ups for phase 1 can be found in the phase 1 document [1]

At the time of publishing, only the group representing the SMARTFIRE SP had submitted Phase-2 results.

3.1 CFD cases

The CFD cases were intended to test the fundamental physical modelling capabilities of the SPs.

On the whole, all the SPs performed well on the Phase 1 CFD test cases. The only case that showed room for considerable improvement was the radiation test case (2000-1-5). This was the only CFD test case that was attempted by any of the SPs in Phase 2. This was attempted by SMARTFIRE using their multi-ray radiation model.

3.1.1 SMARTFIRE: 2000-1-5 Radiation in a 3D cavity.

Introduction

The primary purpose of this test case was to test the radiation model used by the SP. Model predictions are cross compared and also compared with theoretical predictions derived from detailed zone methods [6, 7].

The geometry used for this test case consists of a three dimensional unit cube (1m x 1m x 1m) cavity with three walls with planes $x=1$, $y=0$ and $z=0$ set to a unit emissive power and the three other walls set to zero emissive power. All the walls are considered radiatively black with unit emissivity and the fluid has a unit absorption coefficient. Scattering is neglected. No fluid flow is considered.

Phase 2 Model Configuration

From the results for phase 1 [1] it was apparent that although the six-flux radiation model could produce good results for certain fire cases i.e. non-spreading fires, it was inadequate for other fire applications such as those involving fire spread. While the six-flux model appears capable of representing the average trends within a compartment, it does not produce an accurate representation of local conditions. As part of the phase 2 simulations, the SMARTFIRE multi-ray radiation model is tested to see if this would provide the user with better predictions. While this model is implemented within the current release version of SMARTFIRE it has not been made available to general users via the GUI but can be activated via the INF file.

The multi-ray radiation model [8] is more advanced than the six-flux radiation model as the user may specify as many ray directions as is wished, allowing for a model with a more realistic radiation distribution. The multi-ray model may also be used on unstructured meshes. A drawback of the method is that each ray direction requires a linear solver and as many as 24 ray directions may be required to produce a good radiation distribution.

The multi-ray radiation model was run using the following configurations;

- 1) 6-rays – which is equivalent to the 6-flux model with the rays directed in the coordinate directions
- 2) 24-rays
- 3) 48-rays

The rays are weighted and spread over 4π steradians so that the overall radiation distribution is conserved the rules for doing this are described in Appendix B [8].

Phase 2 Results

The results are compared at three locations and compare the above setups with the theoretical zone model result and the SMARTFIRE six-flux results generated in phase 1 [1].

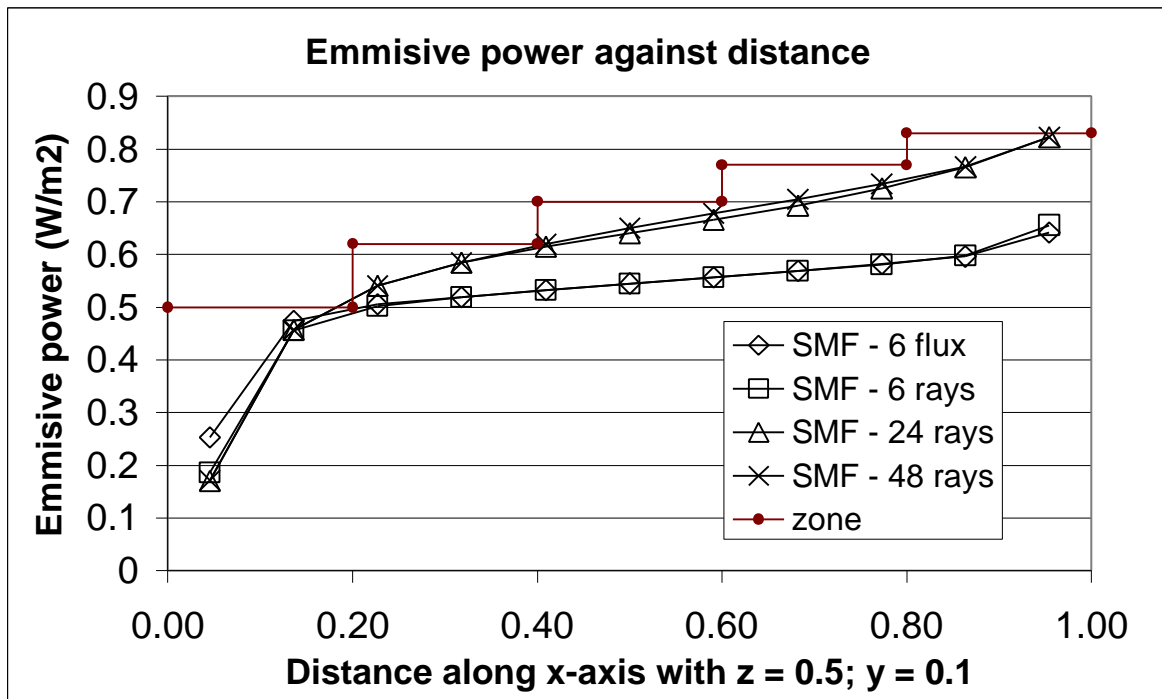


Figure 1 – SMARTFIRE generated emissive power against distance along x-axis for $z = 0.5$; $y = 0.1$ using six-flux and multi-ray radiation models

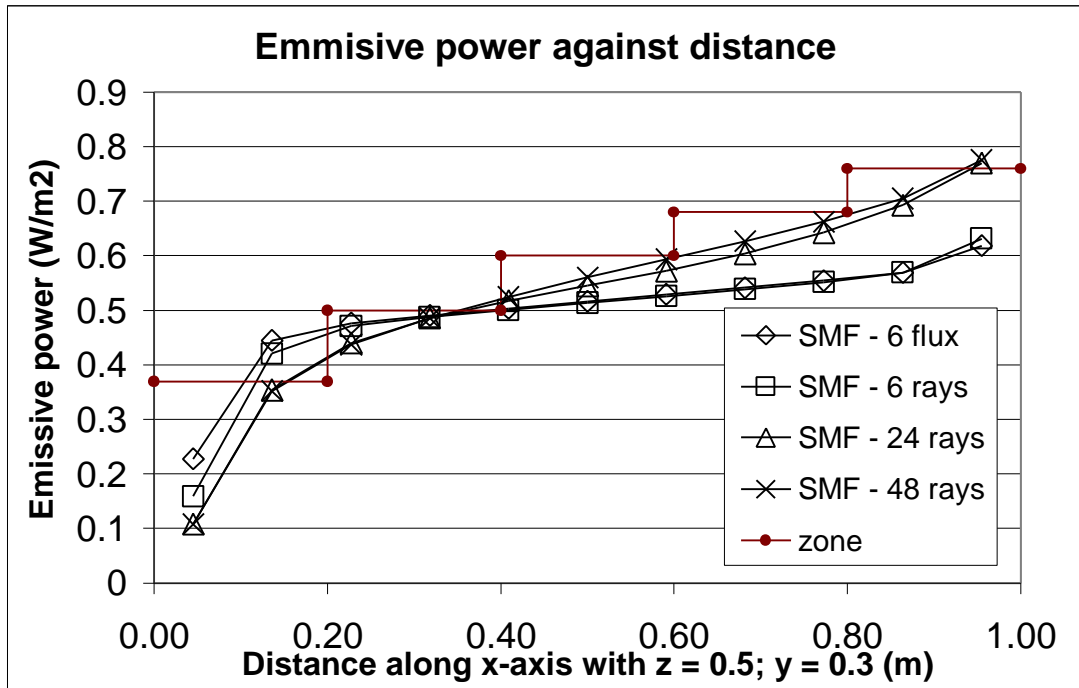


Figure 2 – SMARTFIRE generated emissive power against distance along x-axis for $z = 0.5$; $y = 0.3$ using six-flux and multiray radiation models

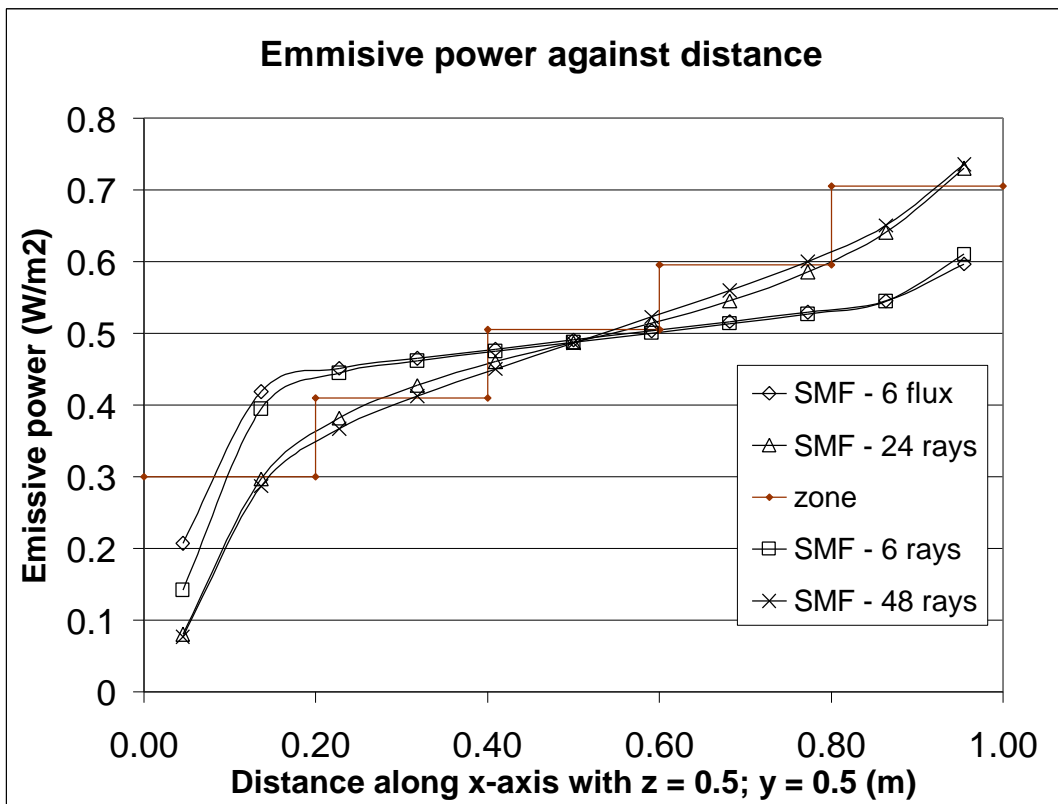


Figure 3 – SMARTFIRE generated emissive power against distance along x-axis with $z = 0.5$; $y = 0.5$ using six-flux and multi-ray radiation models

In Figure 1 to Figure 3 it can be seen that when the multi-ray model is configured with six rays it produces identical results to the SMARTFIRE six-flux radiation model. As found in the phase 1 [1], these results only approximate the radiation distribution within the cavity. When the multi-ray model is configured with 24 and 48 rays, the model produces results that are much closer to the theoretical results. Furthermore, the results generated using 48 rays show only a marginal improvement over the results generated using 24 rays.

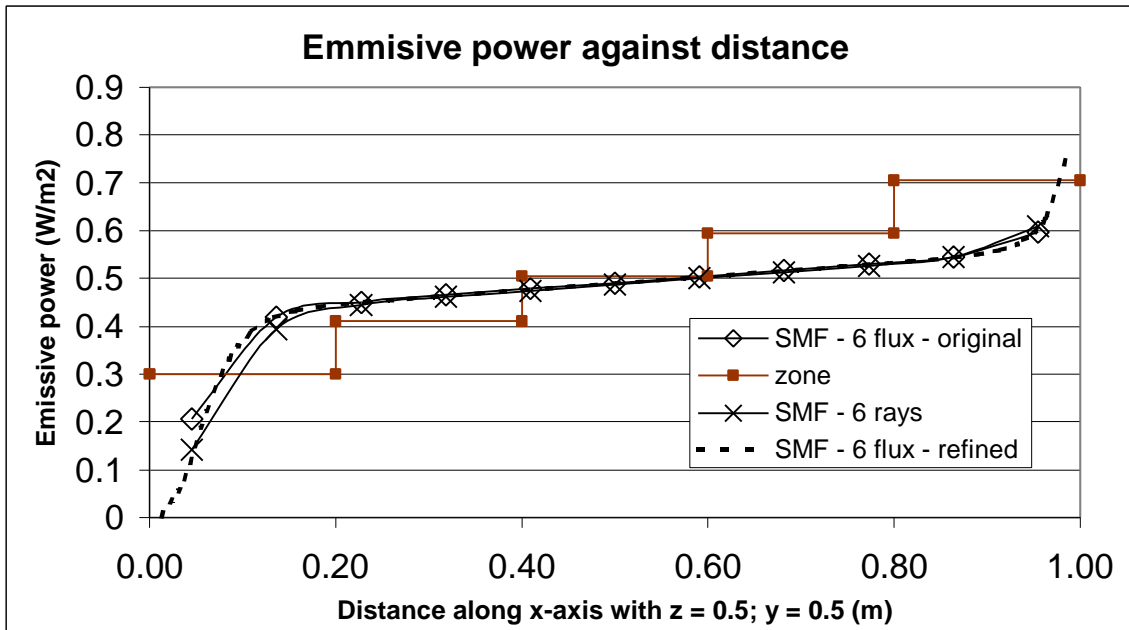


Figure 4 - Refined mesh for SMARTFIRE six-flux radiation model.

The six-flux model was also tested using a much-refined mesh in order to investigate if mesh refinement would improve the predictive capability of the model. The mesh was refined to 41 x 41 x 41 and the case re-run with just the six-flux radiation model. The results for this case are depicted in Figure 4. As can be seen, refining the mesh does not improve the results for the six-flux model.

Finally, the results produced by the SMARTFIRE multi-ray model are compared with the results generated by the CFX discrete transfer radiation model (see Phase-1 report [1]). In comparing the two results it is important to note the difference between the two models. The ray definition used by SMARTFIRE is different to that used by CFX. In SMARTFIRE, the specified number of rays is the number of rays emanating from a nodal point. However in CFX, the number of rays is the number of rays leaving each cell surface. Therefore CFX with 1 ray is approximately equivalent to SMARTFIRE with 6 rays and CFX with 12 rays is approximately equivalent to SMARTFIRE with 72 rays. Also, while the CFX radiation model makes use of a different computational mesh to that used in the flow calculations, the SMARTFIRE multi-ray model uses the same computational mesh for both radiation and flow calculations.

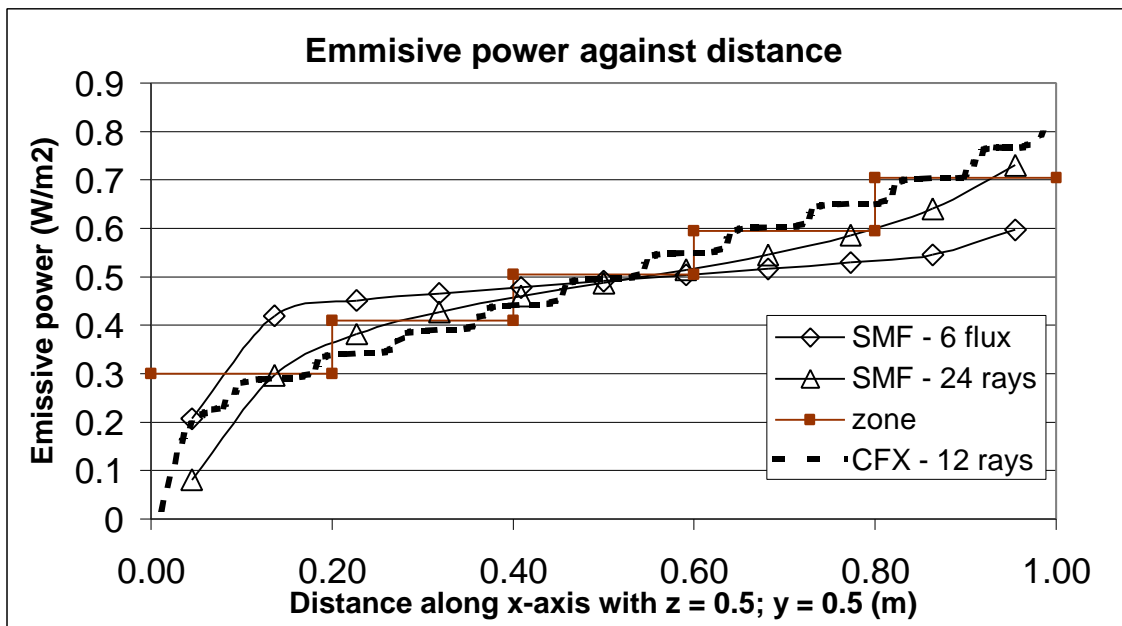


Figure 5 - Comparison of SMARTFIRE radiation models with CFX radiation model

As can be seen from Figure 5, both the CFX and SMARTFIRE radiation models produce a good comparison with the theoretical zone model result. The stepping noted in the CFX results is a consequence of the differences between the CFD mesh and the radiation mesh.

In conclusion, the SMARTFIRE multi-ray radiation model produces better agreement with the theoretical results than the standard six-flux model. It is also apparent that the quality of the results are dependent on the number (and direction) of rays used. When using six rays directed along the co-ordinate axes, the multi-ray model produced identical results to the SMARTFIRE six-flux model. For this particular problem, using 24 rays produced similar results to 48 rays but at much reduced computational cost, approximately half the time in this instance.

While the multi-ray radiation model is computationally more expensive – hence less desirable - than the six-flux model, in situations where radiation plays a key role such as in the modelling of spreading fire, it is essential.

3.2 Fire cases

Several of the fire test cases completed in Phase 1 showed room for improvement. All of the SPs tested could have improved their predictions through the use of a combination of refined meshes, activation of more sophisticated sub-models and the use of more realistic boundary conditions. Two fire cases were submitted for Phase 2, these were the Steckler fire case (2000-2-1) and the LPC007 fire case (2000-2-5). Both these cases were attempted by SMARTFIRE. In this section the results are presented.

3.2.1 SMARTFIRE: 2000-2-1 – Steckler fire case

Introduction

This test case (2000-2-1) was simulated with the prescribed heat release rate model. Test case 2000-2-2 considered the Steckler fire case with combustion model [1]. The volumetric heat source was chosen as there was little difference between the results generated by the combustion model and the volumetric heat source model in Phase-1 [1]. The Steckler case is a standard fire model test case used by a number of field and zone model developers. Its primary purpose is to test the fire models predictive capability in predicting temperature and flow distributions in a small compartment subjected to a steady non-spreading fire. Predictions of several parameters are made and cross compared. Model predictions are also compared with experimental results [9].

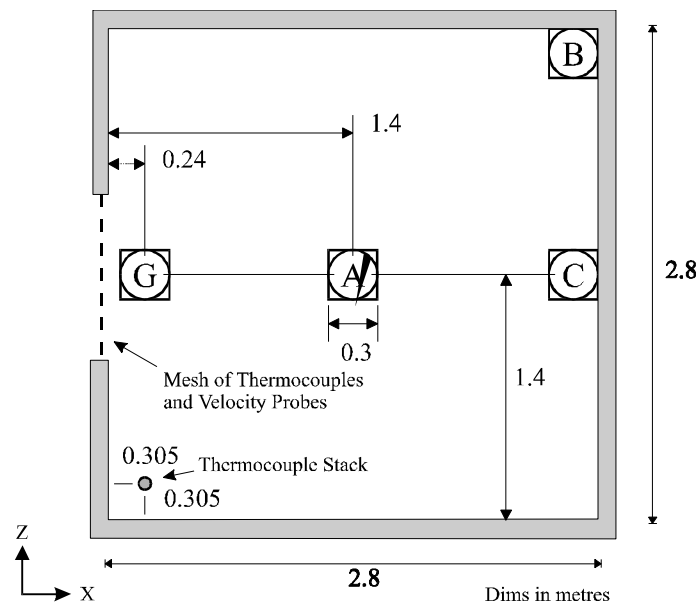


Figure 6 – Configuration of Steckler room

The non-spreading fire was created using a centrally located (position A in Figure 6) 62.9kW methane burner with a diameter of 0.3m. The experiments were conducted by Steckler et al [9] in a compartment measuring 2.8m × 2.8m in plane and 2.18m in height (see Figure 6) with a doorway centrally located in one of the walls measuring 0.74m wide

by 1.83m high. The walls and ceiling were 0.1m thick and they were covered with a ceramic fibre insulation board to establish near steady state conditions within 30 minutes. The door measures 0.74m wide and 1.83m high and is centrally located in one of the walls.

Phase 2 Model Configuration

From the Phase 1 results it was apparent that all the SPs over-predicted the temperatures generated by the fire. This was expected as all the SPs assumed that the walls were adiabatic and perfect radiative reflectors. In the second phase of the validation process SMARTFIRE is used with the multi-ray radiation model and more realistic physical properties and boundary conditions. Finally a more refined mesh is used.

The simulation results presented can be summarised as follows:-

- 1) Phase 1 results for 2000-2-1 (using a simple volumetric heat release rate model).
- 2) As (1) with improved physical properties and improved boundary conditions.
- 3) As (2) with the multi-ray radiation model with 24 rays replacing the six-flux radiation model.
- 4) As (2) with refined mesh and taking advantage of symmetry.

All the cases were run for 200 seconds of simulated time using 200 timesteps of 1 second at which point steady state conditions are achieved.

In cases (1), (2) and (3) the same computational mesh is used; this mesh is composed of 13,020 ($31 \times 20 \times 21$) cells. In case (4) the computational mesh is 49,980 ($49 \times 34 \times 30$) cells; it must also be remembered that only half the domain is modelled as symmetry is used which produces an equivalent cell budget of 99,960 ($49 \times 43 \times 60$) cells.

In set up (1) it was assumed that the walls are adiabatic and perfectly reflecting (emissivity = 0). It was also assumed that the absorption coefficient of the air and gas mixture had a constant value of 0.315.

In set ups (2), (3) and (4) it is assumed that all the walls are composed of heat conducting “common” bricks of 0.1m thickness which have the following material properties: specific heat 840 J/kg.K, thermal conductivity 0.69 W/m.K and density 1600 kg/m³. The wall emissivity is assumed to be 0.8. The model uses turbulent (log-law) momentum and heat transfer at the walls (See SMF Manual [5] for further details). The effect of radiation is also modelled at the wall. The modelling of the heat transfer at the wall can be expressed as:-

$$-\lambda_w \partial T / \partial n \Big|_w = H_c (T_w - T_{\text{gas}}) + \epsilon \sigma T_w^4 - \epsilon \dot{Q}_r''$$

where λ_w is the conductivity of the wall material, T_w is the wall surface temperature, T_{gas} is the air temperature next to the wall, H_c is the convective heat transfer coefficient, ϵ is the wall emissivity and \dot{Q}_r'' is the radiative heat flux at the wall surface.

The absorption coefficient of the air and gas mixture is modelled as

$$a = 0.01, \text{ if } T < 323\text{K};$$

$$a = 0.01 + (3.49/377)(T-323), \text{ if } 323\text{K} \leq T < 700\text{K};$$

$$a = 3.5 + (3.5/700)(T-700), \text{ if } T > 700\text{K}.$$

Phase 2 Results

Comparisons between the above set ups are presented below (Figure 7 - Figure 9). The comparisons are made at two different locations; corner thermocouple stack located in one of the near corners to the doorway and a thermocouple and velocity measuring stack centrally located in the doorway (see Figure 6). The results presented are after 200s of simulated time at which point the results are steady state.

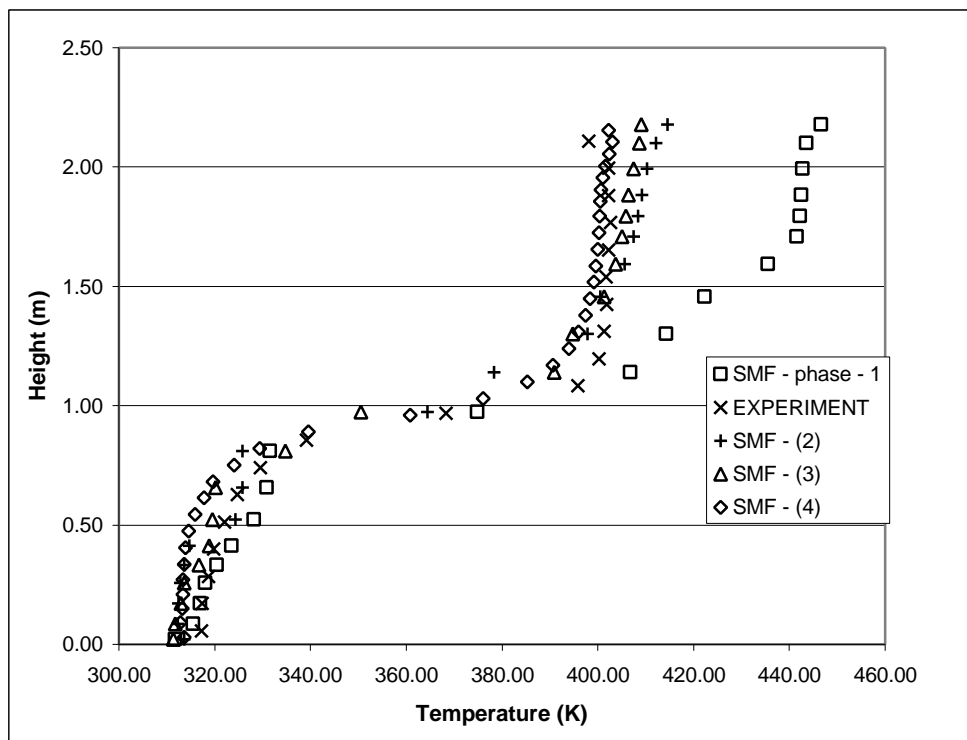


Figure 7 - Corner Stack temperatures produced using the various set ups for SMARTFIRE.

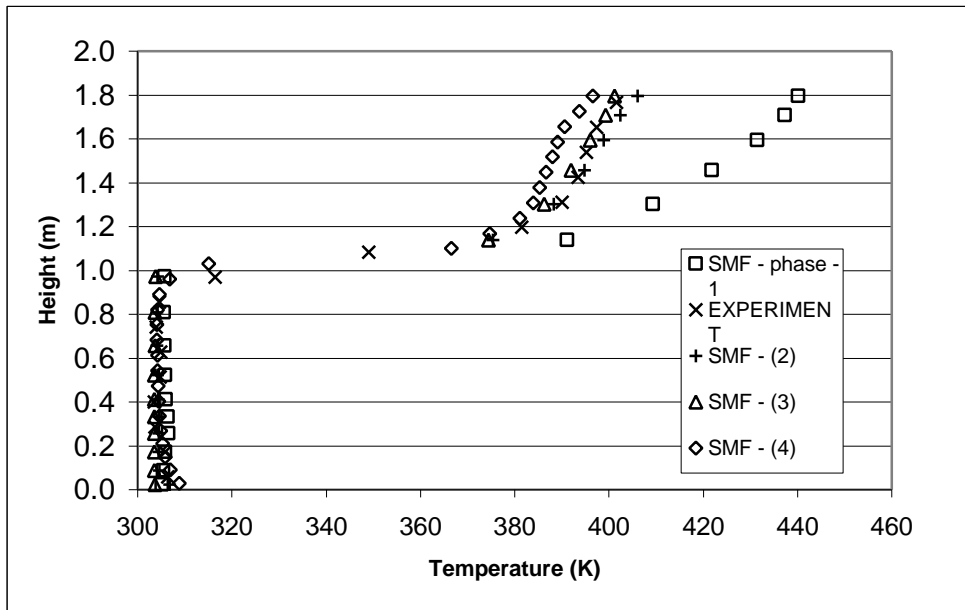


Figure 8 - Comparison of doorway temperatures for Steckler room

Depicted in Figure 7 is the corner stack temperature profile generated by SMARTFIRE using the four model configurations along with the experimental results. Depicted in Figure 8 is the doorway centre temperatures. As can be seen, all three simulations produce a much better reproduction of the temperature distribution within the compartment than the original Phase 1 predictions. Table 1 shows the model estimated upper layer temperature using the values given in Figure 7. Here again we note that the refined models produce a much better representation of the upper layer temperature.

The overprediction produced in the Phase-1 simulations has been greatly reduced by each of the measures. Improving the physical properties and the wall boundary conditions produce the most significant improvement in the results. This has brought the upper layer temperatures down to very close to the observed values. Further improving the representation of the radiation distribution has not lead to a further significant improvement. This is to be expected as the temperatures are rather low and so the heat transfer via radiation is expected to be low. In this case the six-flux radiation model suffices. Finally, refining the mesh (i.e. case 4) leads to only a minor improvement in the model predictions compared with that obtained by using improved material properties and wall boundary conditions (i.e. case 2).

Table 1 - Approximate upper heat layer temperature for Steckler’s room (A74) using the four SMARTFIRE configurations

	Exp	SMF-(1)	SMF-(2)	SMF-(3)	SMF-(4)
Temp (K)	401	442	408	406	400

The location of the hot layer can be estimated by determining where uniform temperatures are established in the upper layer. The height for the hot layers are detailed in Table 2. These represent the height of the bottom of the hot layer from the floor.

Table 2 - Approximate height of the hot layer f for Steckler's room (A74) using the four SMARTFIRE configurations

	Exp	SMF-(1)	SMF-(2)	SMF-(3)	SMF-(4)
Height (m)	1.25	1.6	1.35	1.5	1.4

As the hot layer is not sharply defined, an alternative definition for the height of the thermal interface can be defined as the height with the mid-point temperature. These values are presented in Table 3.

Table 3 - Approximate height of the hot layer f for Steckler's room (A74) using the four SMARTFIRE configurations (alternative definition)

	Exp	SMF-(1)	SMF-(2)	SMF-(3)	SMF-(4)
Height (m)	0.97	1.0	0.97	1.0	0.97

The alternative definition gives a closer comparison for all the models with the experimental values. The first definition suffers from the fact that the models tend to smear the interface and the temperature is still increasing within the hot layer so the exact location of the hot layer is open to interpretation. The alternative definition does not suffer from this open ended interpretation. This second definition was also used by Steckler [9].

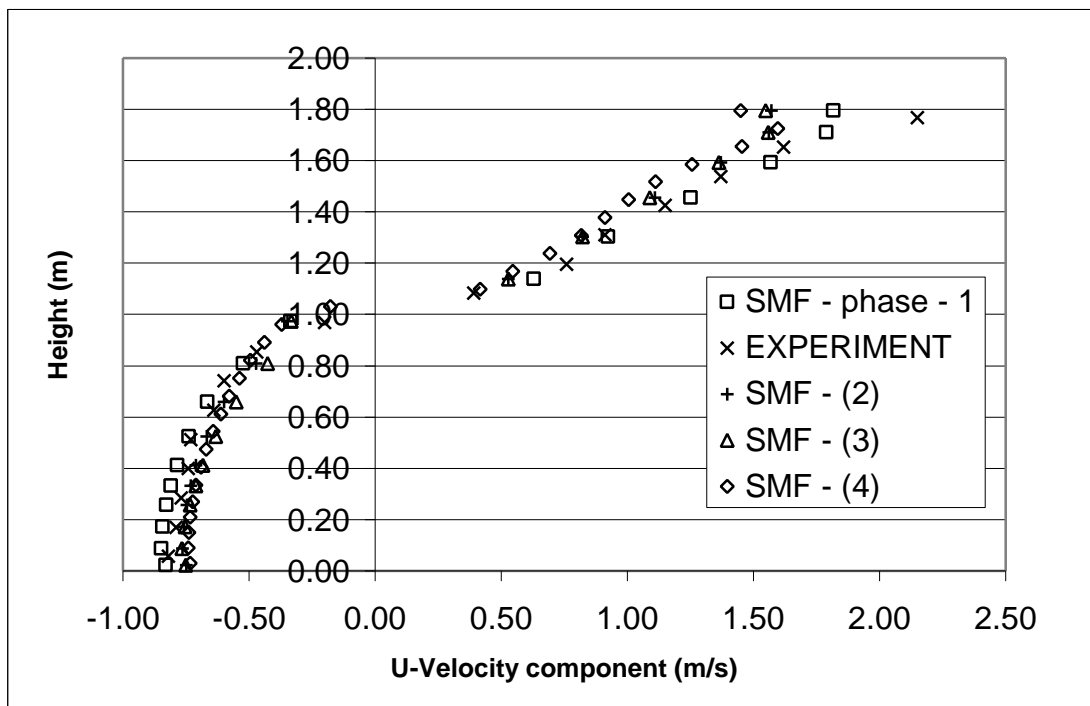


Figure 9 - Comparison of doorway velocity profiles for Steckler room

Depicted in Figure 9 is the horizontal velocity distribution along the centre vertical axis of the doorway. As can be seen all four model configurations produce a very good representation of the velocity distribution. Each of the model configurations predict that the neutral plane height will be slightly above 1m, which is approximately the value obtained from the experiment.

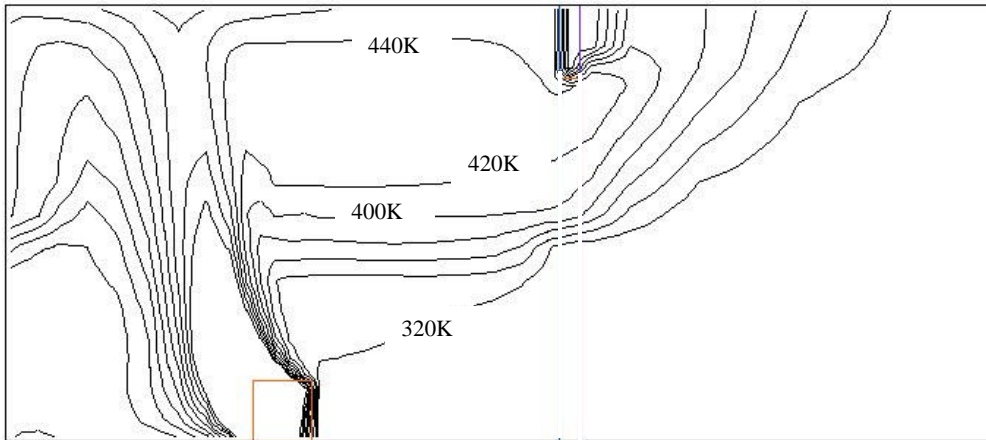


Figure 10 - Temperature contour plot produced by SMARTFIRE using the heat source model with phase-1 conditions.

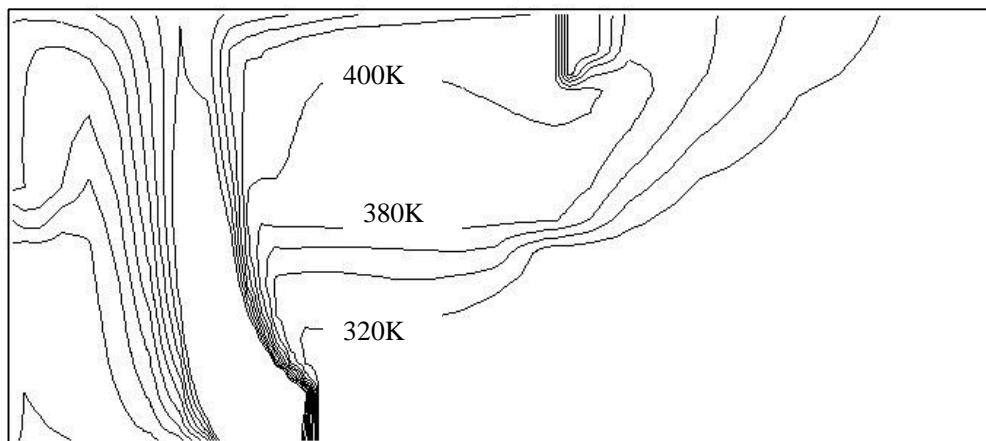


Figure 11 - Temperature contour plot for Case 2

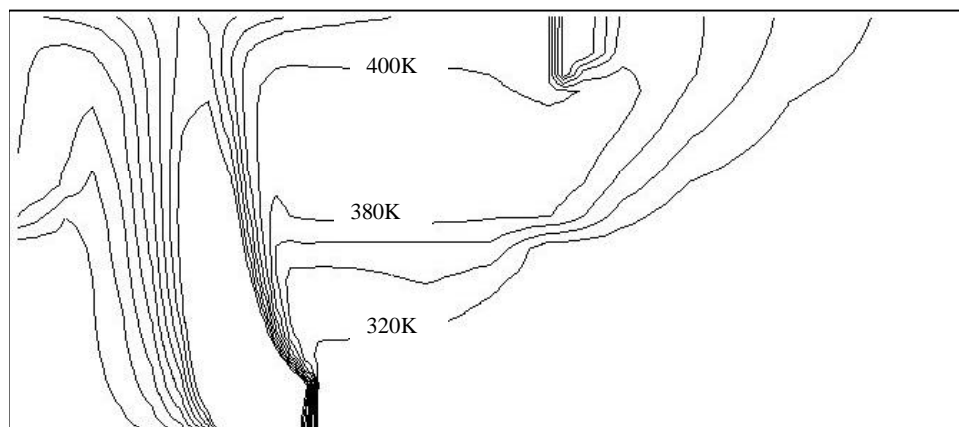


Figure 12 -- Temperature contour plot for Case 3

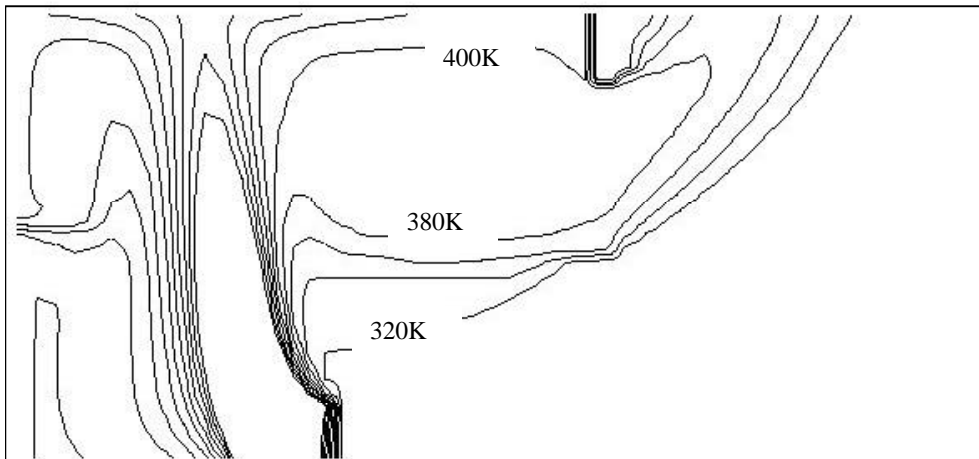


Figure 13 - - Temperature contour plot for Case 4

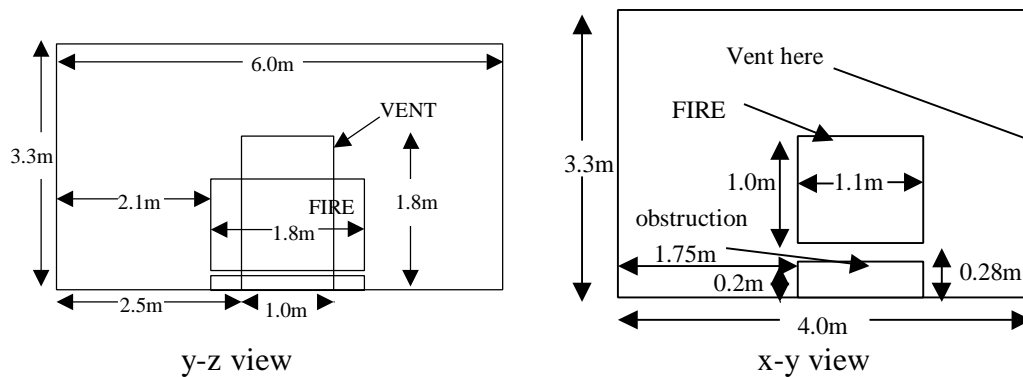
Depicted in Figure 10 to Figure 13 are temperature contour plots along the centre of the compartment for each of the four model configurations. As can be seen, each of the refined model configurations produces similar temperature distributions

From the above results it is clear that the Steckler room predications are improved by the introduction of the improved boundary conditions and material properties. For this particular problem there is no real advantage in using the multi-ray radiation model over the six flux model. Furthermore, once the improved boundary conditions and material properties are used, grid refinement does not further significantly improve the quality of the predictions.

3.2.2 SMARTFIRE: 2000-2-5 – LPC007 case

Introduction

This test case arises from a fire test conducted by the Loss Prevention Council (LPC) [10]. The test is a burning wood crib within an enclosure with a single opening. The test compartment is illustrated below and had a floor area of 6m x 4m and a 3.3m high ceiling. The compartment contained a doorway (vent) measuring 1.0m x 1.8m located on the rear 6m x 3.3m wall. The walls and ceiling of the compartment were made of fire resistant board (Asbestos) which were 0.1m thick. The floor was made of concrete. A steel obstruction measuring 1.1 x 1.8 and 0.2 m high was located on the floor below the fire. The corner thermocouple stack is located at 0.57m away from the side wall and 0.5m away from the front wall containing the vent. The plume temperature measurements were taken at 3.0m away from the side wall and 2.392m away from the back wall of the compartment.



The heat release rate (\dot{Q}) is given by the following calculation (see equation 1).

$$\dot{Q} = c \cdot \Delta H_c \cdot \dot{m} \quad (1)$$

The efficiency factor (c) and heat of combustion (ΔH_c) were given as $c=0.7$ and ΔH_c is 17.8 MJ/kg for burning wood with a 10% moisture content and the mass loss rate (\dot{m}) (kg/s) for the wood crib is presented in the table below. It is assumed that the fuel molecule is $\text{CH}_{1.7}\text{O}_{0.83}$. The mass loss rate is given in Table 4 below.

Table 4 - Fuel mass loss rate used in test case 2000-2-5

Time(s)	0	150	450	460	1650
\dot{m} (kg/s)	0	0.01835	0.18636	0.1978	0.1978

See Appendix E1 and E2 for further set-up details.

Phase 2 Model Configuration

The basic configuration of the model is as in Phase 1. Phase 1 included the use of the combustion model. In Phase 1 this case proved difficult to converge and the numerical

predictions were prematurely terminated. As a result, only part of the experimental data was utilised. It was felt that the difficulty in Phase 1 was caused in part by the artificial nature of the boundary conditions i.e. the use of adiabatic boundary conditions and the use of perfectly reflecting walls (emissivity = 0). The absorption coefficient was assumed to be a constant of 0.315.

In the Phase 2 simulations the wall boundary conditions were more accurately modelled, better physical properties were used and the multi-ray radiation model was used. In total two additional simulations were performed.

The same mesh was used for all the cases, the mesh had a cell budget of 26,040 (31 x 24 x 35). The case was run using 180 x 5-second timesteps to give an overall simulation time of 900s.

The physical properties detailed in Table 5 were used for both the phase-2 simulations. The Phase-1 model used the same properties for air but all the solids were assumed to be non-conducting.

Table 5: Material properties used in test case 2000-2-5

Mat. Name	Density	Viscosity	Conductivity	Specific heat
Air	Ideal Gas (molecular weight = 29.35)	1.798E-05 + turbulent value	0.02622	1007.0
Asbestos	577	1E+10	0.15	1050.0
Concrete	2300	1E+10	1.4	880.0
Steel	7850	1E+10	45.8	460.0

The first case involved the following configuration:

The boundary conditions were modelled more accurately using heat-conducting walls that took into account the physical properties of the wall (asbestos). The properties of the floor (concrete) and the steel obstruction were also taken into account.

The wall emissivity is assumed to be 0.8. The model uses turbulent (log-law) momentum and heat transfer at the walls (See SMF Manual [5] for further details). The effect of radiation is also modelled at the wall. The model of the heat transfer at the wall can be expressed as:-

$$-\lambda_w \partial T / \partial n \big|_w = H_c (T_w - T_{\text{gas}}) + \epsilon \sigma T_w^4 - \epsilon \dot{Q}_r''$$

where λ_w is the conductivity of the wall material, T_w is the wall surface temperature, T_{gas} is the air temperature next to the wall, H_c is the convective heat transfer coefficient, ϵ is the wall emissivity and \dot{Q}_r'' is the radiative heat flux at the wall surface. Currently there is no history term to account for the for the heat accumulation in the wall. This will have the effect of not removing as much heat as expected during the growth phase of the fire and removing too much heat during the decay phase of the fire.

The SMARTFIRE gaseous combustion model was used. A volumetric mass loss source was used to represent the burning of the wood crib whose time dependent curve of mass loss rates was provided by the LPC report (see Table 4 above). The combustion efficiency was assumed to be 0.7. The heat of combustion used in the simulations was 17.8 MJ/kg.

A simple one-step global chemical reaction is adopted in the gaseous combustion model, i.e.,



where F is the fuel, O is the oxidant, P is the product and s is the stoichiometric ratio of oxygen to fuel. The heat released through the consumption of one unit mass fuel is denoted by $H(\text{J/kg})$.

Four scalar variables are used in the combustion model. They are mixture fraction(f), mass fraction of fuel(m_f), mass fraction of air(m_a) and mass fraction of products(m_p). Two additional scalar governing equations are introduced for the fuel mass fraction m_f and the mixture fraction f . This is activated by using a keyword COMBUSTION in PROBLEM DEFINE in the inf file. The air mass fraction m_a and the products mass fraction m_p are algebraically calculated in terms of the following algebraic equations

$$m_a = 1 - m_f - (f - m_f) / f_s \quad (2)$$

$$m_p = 1 - m_f - m_a \quad (3)$$

rather than differential equations, where f_s is the stoichiometric value of f , defined by $f_s = 1 / (1 + s)$.

The mixture fraction is a conserved scalar and hence there is no source term in its governing equation. The source term in the governing equation for mass fraction of fuel employs the eddy dissipation concept, i.e.,

$$R_f = A \min(\bar{C}_f, \bar{C}_o / s) \frac{\mathbf{e}}{k} \quad (4)$$

[4], where R_f is the fuel consumption rate(kg/s), A is a constant, min represents the minimum of two numbers, \bar{C}_f is the time-averaged fuel concentration, \bar{C}_o stands for the time-averaged oxidant concentration, k and \mathbf{e} are the turbulent kinetic energy and the turbulence dissipation rate respectively.

The radiation absorption coefficient for both radiation models was assumed to take the following form:-

$$a = 0.01, \text{ if } T < 323\text{K};$$

$$a = 0.01 + 0.305/377(T-323), \text{ if } 323 \leq T < 700;$$

$$a = 0.315 + 0.315/700(T-700), \text{ if } T > 700.$$

The second case involved the following configuration:

As the first case but with the six-flux radiation model replaced with the multi-ray radiation model using 24 rays (identified as SMF-MR). See section 3.1.1 for details of the multi-ray radiation model.

Phase 2 Results

The results for the plume thermocouple and room corner thermocouple stack are shown in Figure 14 and Figure 16. The lower (L) and higher (H) values refer to measurements at 1.5m and 3.0m above the ground respectively. In the graph keys SMF refers to case 1 (i.e. improved boundary conditions and material properties with six-flux model) and SMF-MR refers to case 2 (i.e. improved boundary conditions and material properties with multiray radiation model).

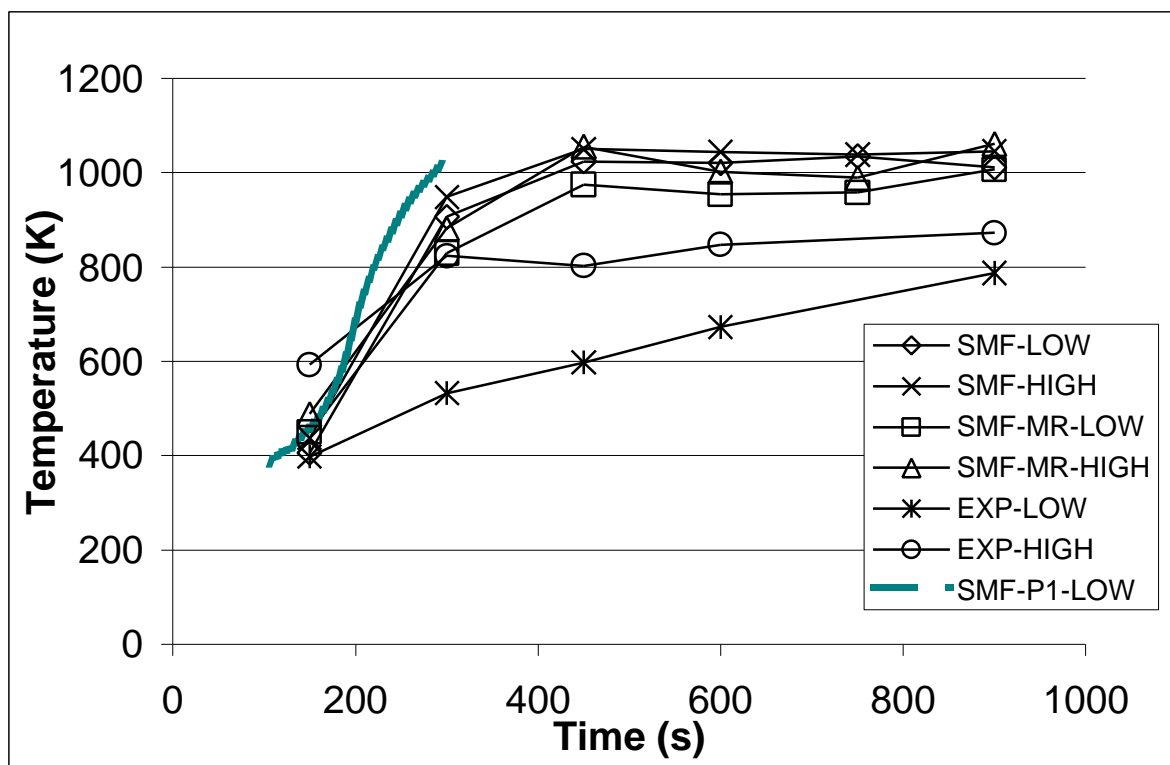


Figure 14 - Predicted and measured Corner Stack Temperatures at 1.5m (L) and 3.0m (H) above the floor for the LPC test case

With the improved Phase 2 model specifications, it was possible to simulate the entire duration of the experiment. The convergence problems noted in Phase 1 were completely removed. Furthermore, examination of the corner stack temperature predictions reveals that the improved boundary conditions and physical models reduced the temperature predictions compared to the phase-1 results bringing them closer in line with the measured values. In addition, the incorrect behaviour noted in Phase 1 where the temperature predictions in the lower region of the room exceed the temperatures in the higher region is corrected. However, the level of stratification observed in the predicted results is not as great as that observed in the experiment. The multi-ray model produces a

slightly greater stratification between the upper and lower temperatures than that produced using the six-flux model.

Both of the Phase 2 cases overpredict the experimental values with the results generated using the multi-ray model being slightly closer to the measured results. Differences between the multi-ray model and the experimental results for the high measuring location are as high as 30%, while for the low measuring location, the error is as high as 63% (see Figure 15). For the six-flux model, the maximum errors are 31% and 71% respectively. The experimental trends in the upper temperatures are reproduced well by the numerical predictions. These temperatures tend to increase until about 300 seconds into the fire and then remain approximately constant. The numerical predictions follow this trend but the peak is reached at approximately 425 seconds. The experimental trends in the lower temperatures show a continual increase over the entire duration of the experiment. However, the numerical predictions for the lower temperatures follow those of the upper temperatures.

The noted overprediction could be due to inaccuracies in the experimental data and deficiencies in the model assumptions such as assuming a constant wall emissivity of 0.8.

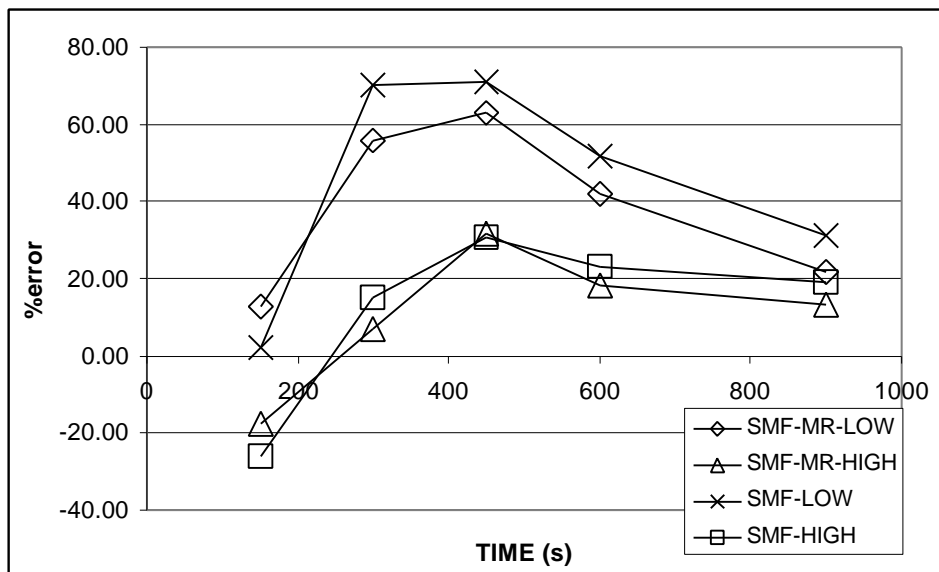


Figure 15 – Error (%) in the SMARTFIRE predictions using the six-flux model for the corner stack in test case 2000-2-5

The plume stack temperature predictions are depicted in Figure 16. They follow the general experimental trend of a peak followed by a dip (see Figure 16). The SMARTFIRE simulation demonstrates that this trend is mainly caused by the changes of the fire plume shape. After the initial phase of fire growth, the fire becomes quite large and the hot combustion products accumulate beneath the ceiling creating a gradually deepening hot layer. In conjunction with the fresh air being entrained into the compartment by the fire, the downward movement of the hot upper layer pushes the fire plume back so that it tilts away from the window towards the rear wall. Thus, the fire

plume has shifted away from the central vertical line of the crib. Since this line – and hence the measuring devices - are not in the centre of the fire plume, the temperatures along it predicted and measured are reducing after they reach the peak value.

It is also notable that the experimental measurements indicate that the plume is hotter at the top than at the lower level that is suggested by the model predictions. This could be due the combustion behaviour with combustion occurring more in the upper layers of the compartment. It was noted in the experiment that some flaming combustion occurred outside the compartment. This may explain the higher temperatures numerically predicted within the compartment as all the combustion is assumed to have occurred within the compartment. Another source of error is the presence of the wooden crib. This would act as an obstruction, which is dynamically changing throughout the combustion process. This obstruction effect is ignored in the numerical modelling as it is difficult to model this changing shape. The obstruction would have some effect on the airflow within the compartment particularly into the plume.

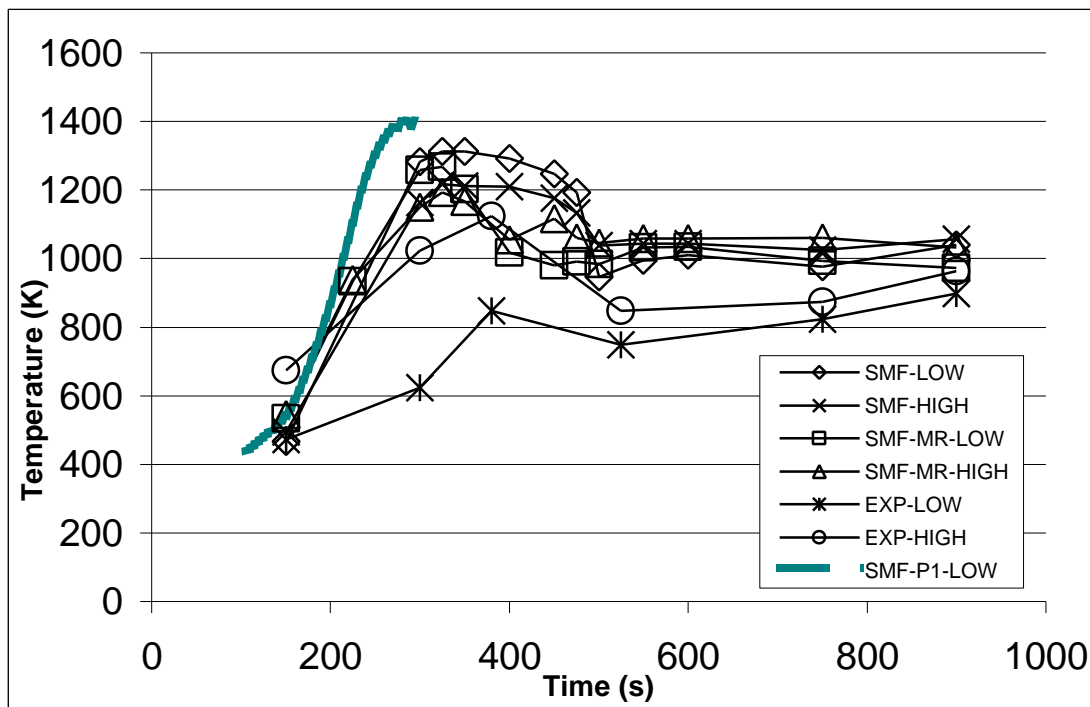


Figure 16 - Plume stack temperature predictions for SMARTFIRE for test case 2000-2-5

There is a distinct difference in the plume behaviour for the six-flux model and the multi-ray radiation model (24 rays). The peak in temperature lasts longer for the six-flux model but it is difficult to say which of the model predictions is better in this particular simulation.

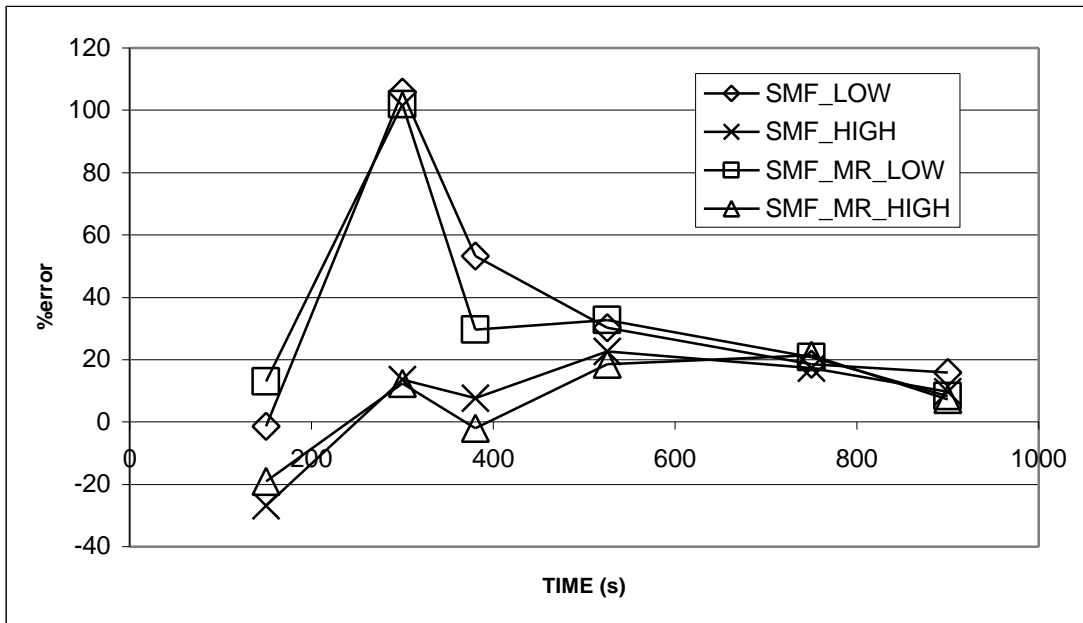


Figure 17 - Error (%) in the SMARTFIRE predictions using the multi-ray model for the corner stack in test case 2000-2-5

As with the corner measurements, both of the plume simulations overpredict the experimental values with the results generated using the multi-ray model being slightly closer to the measured results. Maximum differences between the multi-ray model and the experimental results for the high measuring location are 21%, while for the low measuring location, the error is 100% (see Figure 17). For the six-flux model, the maximum errors are 27% and 106% respectively.

The improved boundary conditions and wall properties have greatly improved the quality of the model predictions. The numerical predictions follow the general experimental trends while overpredicting the experimental results. The discrete transfer radiation model has marginally improved the quality of the numerical predictions but at the cost of increased computational time.

CONCLUDING COMMENTS

The second phase of the testing programme has been successfully completed. In studying the results generated in Phase 2 it is important to note the following points:

- 1) The results generated and comments made only refer to the software actually used in the trials. This should not simply be taken to mean the product name but also the release number and version number of the software.
- 2) Only the SMARTFIRE SP participated in Phase 2.
- 3) Only three test cases were selected for Phase 2, these were the radiation test case 2000-1-5, the Steckler room fire case 2000-2-1 and the LPC fire case 2000-2-5.
- 4) While the Phase 1 simulations did not make use of the most sophisticated physics models available in each of the SPs, the Phase 2 simulations are intended to explore the benefits of using more sophisticated physics models and finer computational meshes.
- 5) The series of trials undertaken in this project should not be considered to be definitive. They have been selected as a basis for exploring the potential of the benchmarking process. It is intended that additional tests should be added to the suite of test cases.

From the Phase 2 analysis it has been demonstrated that the SMARTFIRE SP is capable of producing improved results over those predicted in the Phase 1 testing regime. The Phase 1 testing regime was essential to allow comparison between different computer codes without the bias of the user or specialist features that may exist in one code and not another. In Phase 2 the user was free to perform the test using the best modelling features available in the code to best represent the scenario being modelled. In this way it was hoped to demonstrate that in addition to achieving a common minimum standard of performance, the SP's were also capable of achieving improved agreement with the experimental or theoretical results.

Predictions for the radiation test case (2000-1-5) using the SMARTFIRE multi-ray radiation model with 24 rays, showed considerable improvement over the results generated in Phase 1. The results from this simulation indicate the greater inherent accuracy that the multi-ray radiation model has over the simpler six-flux model. It is important to note that the greater degree of accuracy offered by the multi-ray model may not manifest itself in producing more accurate fire predictions. Whether or not the multi-ray radiation model will make a significant difference in a fire simulation depends on the nature of the case being examined.

In the Phase 1 simulations, all the SPs predictions for the Steckler room fire case (2000-2-1) failed to accurately reproduce the measured temperatures, but successfully captured the overall trends. The results for Phase 2 showed that considerable improvement could be achieved by a more sophisticated treatment of the wall boundary conditions and more accurately representing the material properties. While further improvement could be

achieved through the use of the multi-ray model and mesh refinement, these were insignificant in comparison.

In Phase 1, it was not possible to generate converged solutions of the LPC-007 case (i.e. 2000-2-5) beyond 300s. This was thought due to the nature of the boundary conditions selected for Phase 1. In Phase 2, with a more sophisticated treatment of the wall boundary conditions - which included a heat loss calculation - it was possible to generate converged solutions for the entire duration of the experiment. While errors in the numerical predictions persisted, the numerical predictions were able to reproduce most of the observed trends in the experimental results.

In studying the outcome of the Phase 2 test cases, it is clear that by activating sophisticated physics models, the SP tested was capable of generating improved predictions in all of the cases examined. While this may seem an intuitively obvious result, it is a necessary demonstration of the capability of the fire modelling tool that this can be done in a measurable and reproducible manner.

Furthermore, these results should not be treated in isolation but taken within the context of the Phase 1 findings. A significant conclusion from the Phase 1 predictions was that within the limits of the Phase 1 testing regime and taking into consideration experimental inconsistencies and errors, all three SPs were capable of producing reasonable engineering approximations to the experimental data, both for the simple CFD and fire cases. With the completion of the Phase 2 testing, this statement is somewhat strengthened - at least for the SP tested in Phase 2.

The concept and testing protocols developed as part of this project have been shown to be a valuable tool in providing a verifiable method of benchmarking and gauging the basic and advanced capabilities of CFD based fire models on a level playing field. To further improve the capabilities of the approach, it is recommended that additional test cases in the two categories, theoretical and experimental, be developed and several of the fire cases be refined.

In addition, a modification to the testing procedures is suggested that would reduce the burden and cost of performing the testing by the test organisation. While all of the test cases using all of the codes were run by a single organisation – in this case FSEG – the code developers also were requested to run an independent selection of the test cases as specified. This was necessary to verify that the results produced in this report are a true and fair representation of the capabilities of the various software products under the specified test conditions. This has proven to be quite useful as it brings the developers into the benchmarking process and it eliminates issues concerning fairness and biased reporting of results. However, if this process is to become a mandatory requirement, the testing organisation will have a considerable amount of work to do if it is to run every software product and its various upgrades through each of the test cases. In order to reduce the cost of testing, it is suggested that the test organisation should only perform the random testing and require the software developers to run and submit all of the test cases.

It is finally recommended that the principles and procedures developed in this project be adopted in some form as a quality measure of fire modelling software that is intended for use in the U.K. for design purposes.

References

1. Grandison, A. J., Galea, E.R. and Patel, M.K., "Fire Modelling Standards/Benchmark, report on Phase 1 Simulations.", University Of Greenwich report for Fire Research and Development Group, Home Office, March 2001.
2. FSEG web site – http://fseg.gre.ac.uk/fire/fire_modelling_standards/index.html
3. `CFX4, Version 4.2', AEA Technology. Harwell, England.
4. H. I. Rosten, D. B. Spalding and D. G. Tatchell, 'PHOENICS: A General-Purpose Program for Fluid-Flow, Heat-Transfer and Chemical-Reaction Processes', in Proceedings of the 3rd International Conference on Engineering Software, 639-655 (1983).
5. Galea E., Knight B., Patel M., Ewer J., Petridis M., and Taylor S., "SMARTFIRE V2.01 build 369D, User Guide and Technical Manual", SMARTFIRE CD and bound manual, 1999.
6. Larsen, M. E., "Exchange Factor Method and Alternative Zonal Formulation for Analysis of Radiating Enclosures Containing Participating Media", Ph. D. Thesis, University of Texas, Austin, 1983.
7. Fiveland, W. A., "Three-Dimensional Radiative Heat-Transfer Solutions by the Discrete-Ordinates Method", J. Thermophysics, Vol 2 (4), pp309-316, October 1988.
8. Jia, F., "The Simulation of Fire Growth and Spread within enclosures using an integrated CFD fire spread model.", PhD Thesis, University of Greenwich, 1999.
9. Steckler, K.D, Quintiere, J.G and Rinkinen, W.J., "Flow induced by fire in a compartment", NBSIR 82-2520, National Bureau of Standards, 1982.
10. Glocking, J.L.D, Annable, K., Campbell, S.C. "Fire Spread in multi-storey buidings – 'Fire break out from heavyweight unglazed curtain wall system – Run 007' ", LPC Laboratories rep. TE 88932-43, 25 Feb 1997.